5-10 MEV INDUSTRIAL HIGH POWER ELECTRON ACCELERATOR

M.Tiunov, V.Auslender, V.Cheskidov, M.Karliner, G.Kuznetsov, I.Makarov, G.Ostreiko, A.Panfilov, N.Romashko, V.Tarnetsky, V.Tkachenko, BINP, Novosibirsk, Russia

Abstract

This paper presents a project of high power linear accelerator for industrial applications. The accelerator has a modular structure and consists of the chain of accelerating cavities, connected by the axis-located coupling cavities with coupling slots in the walls. Main parameters of the accelerator are: operating frequency of 176 MHz, energy of electrons of 5-10 MeV depending on number of accelerating cavities, average beam power up to 300 kW. The required RF pulse power can be supplied by tetrode EIMAC 4CM2500KG or diacrode TH628.

1 INTRODUCTION

Recently the interest was aroused in radiation X-ray technologies because of the high penetration ability of X-rays. It is especially important for pasteurization of wide spectrum of food products, disinfection of mail deliveries, and other applications. However, because of low efficiency of X-ray conversion for electrons with energy within the range below 5 MeV, the intensity of X-rays required for some industrial applications can be achieved only when the beam power exceeds 300 kW.

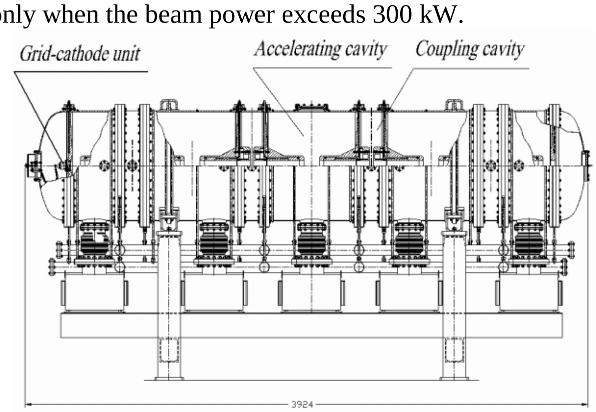

Figure 1: General view of accelerator.

Figure 1 represents the general view of a new efficient electron accelerator for electron energy of 5 MeV and beam power up to 300 kW. The electrons are accelerated in the low frequency multi-resonator standing wave structure with axis-disposed coupling resonators. This design makes it possible to decrease power losses in each resonator comparing with the single-resonator accelerator (at the same average beam power level) and to increase the electron efficiency of the accelerator [1]. The electron beam is injected by triode RF-gun formed by a cathode-grid unit and the first accelerating gap. This concept permits to sufficiently simplify the beam injection system. To realize this concept one has to solve the following problems:

- achievement of the required value of the pulse beam current at relatively low electric field strength in the accelerating gaps comparing with the single-resonator accelerator;
- high-efficient cooling of the accelerating structure's resonators;
- multipactor suppression;
- lossless transportation of a powerful electron beam through the accelerating structure without usage of electro- and magnetostatic lenses.

Solution of these problems will allow us to sufficiently simplify the design and reduce the cost of accelerator respectively, as well as to improve its reliability and reduce the maintenance charges.

The report briefly describes possible ways to solve these problems.

2 GRID-CATHODE UNIT

The beam injection system of the accelerator described (see Fig. 1) must provide the pulse electron current up to 5 A. The amplitude of electric field strength in the grid's plane will be up to 60 kV/cm. The cathode with diameter of 20 mm and area of 3 cm^2 is made of LaB_6.

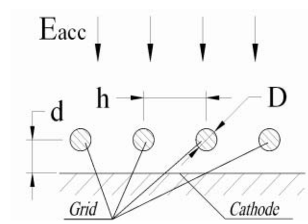

Figure 2: Scheme of grid-cathode unit.

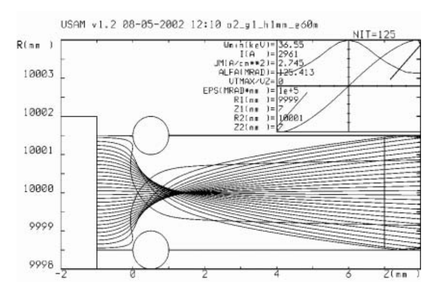

Figure 3: One cell of grid-cathode unit.

Figure 2 represents the scheme of the accelerator's cathode-grid unit. The main geometric parameters of the unit are: the cathode-grid gap d, step of the grid h, and diameter of wires D. The computer optimization of these parameters was carried out by SAM program package [2].

The results given below were obtained using these optimal values.

Figure 3 represents the results of computer simulation of a one cell of the grid-cathode unit in the case of equal potentials of cathode and grid. Figure 4 represents the calculated dependencies of average density of current emitted from cathode-grid unit, relative transverse velocity of electrons in the grid's plane, and relative current falling on grid depending of potential difference between grid and cathode.

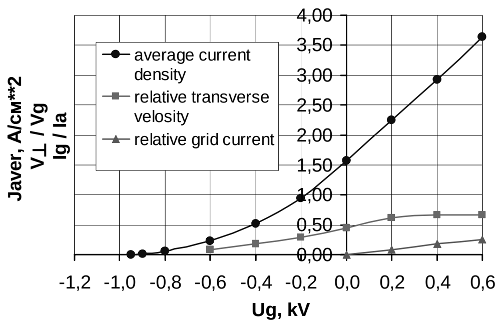

Figure 4: Dependence of average current density, relative transverse velocities and relative grid current on grid-cathode potential.

3 ACCELERATING STRUCTURE

Let us consider the design of the accelerating structure that is presented in Fig.1 in more detail. It is assembled of four identical units (biperiodic structure period) and two end-walls.

Figure 5 represents a period of accelerating structure operating at $\pi/2$ mode, the coupling coefficient is about 10%.

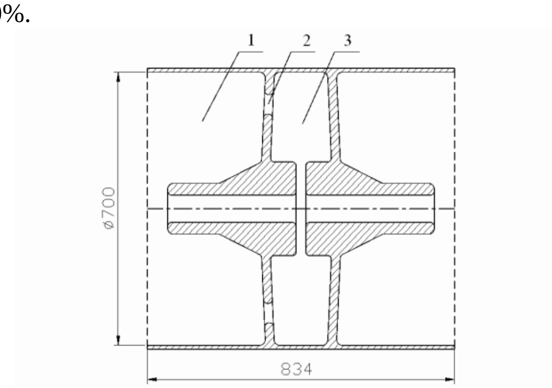

Figure 5: Accelerating structure period with axis-disposed coupling cavity: 1 – accelerating cavity, 2 – coupling slot, 3 – coupling cavity.

This structure advantages are: simple design, convenient cooling, and high resistance to the thermal deformation. It is supposed to coat the inner cavity surfaces by titanium nitride for the multipactor suppression.

In order to create the required accelerating gradient enough for reaching 5 MeV energy of electrons in the accelerating structure, we need about 0.63 MW of RF pulse power. Limiting the power level for creation of the accelerating gradient by 0.8 MW (decrease of Q-factor in 10% due to influence of coupling slots and in 15% due to roughness of surface, etc.). With power supply of 2.8 MW, we can transfer about 2 MW to the beam и can reach electron efficiency of more than 70%. Such RF power can be generated by tetrode EIMAC 4CM2500KG or diacrode TH628.

Accepting 300 kW as an average beam power, we can set duty factor of 15%. In this case the power losses in every unit of accelerating structure (see Fig. 5) will be about 30 kW of average power. The heating of resonators is the main factor that causes the shift of the eigenfrequencies of the structure's resonators, so the efficient cooling of resonators is a must.

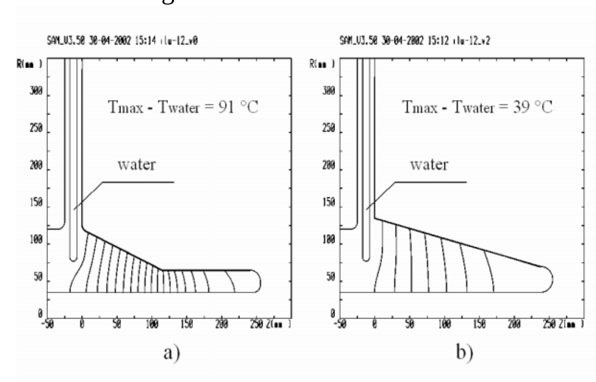

Figure 6: Temperature map of central parts of resonators having two different forms. The isothermal curves show the temperature difference of 5°C.

The possibility of cavity cooling by heat transfer of the central part and radial water channels inside resonators' discs was studied. Figure 6 represents the results of simulation by SAM program of the temperature distribution for two geometries of the central part. Figure 6a shows that this cooling system is not efficient for this geometry. The geometry shown in Fig. 6b is cooled much more efficiently, but this resonator version has less shunt impedance (by 10%). So the first variant has been chosen (see Fig. 6a), but the additional water pipes should be soldered to the central part of the resonator to efficiently cool this system.

4 BEAM DYNAMICS

Computer simulation of the beam dynamics from the grid to the accelerator output was performed in long-wave approximation using SAM code. The transverse velocity spread of electrons due to scattering on the microlenses formed by grid mesh (see Figs. 3,4) has been taken into account. This led to accelerator's aperture increase in comparison with single-gap variant.

Figure 7 represents the results of beam dynamics simulation of the accelerating structure for energy of 5 MeV. The trajectories of electrons started from the cathode edge at different starting phases are shown considering the initial spread of transverse velocity. The simulations proved that there is a possibility to avoid the usage of magnetic focusing elements for the successful transportation of the beam.

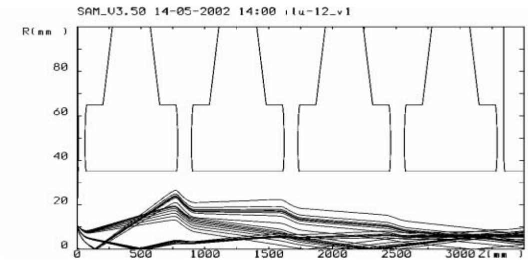

Figure 7: Results of beam dynamics simulation of 5 MeV accelerating structure.

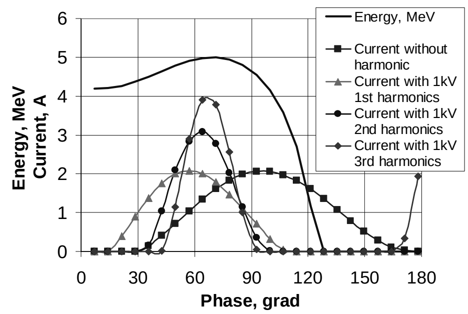

Figure 8: Dependence of electron energy and form of micropulse on starting phase of acceleration.

Figure 8 shows the calculated initial acceleration phase (on grid's plane) dependence of final electron energy at the accelerator's output and the resulting micropulse form. To improve the electron energy spectrum one can apply a constant biasing voltage and an additional biasing RF voltage of either basic, second or third harmonics with appropriate phase shift to the cathode-grid gap.

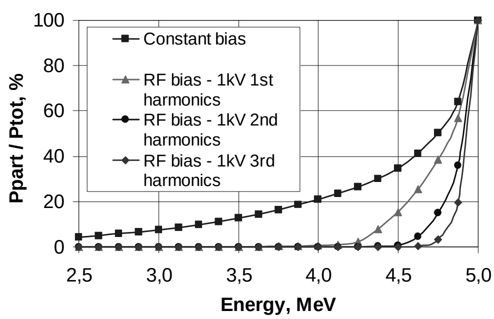

Figure 9: Spectrum of electron energy without and with RF biasing voltage.

Figure 9 represents the calculated energy spectrum of electrons after acceleration using constant cathode-grid bias and with additional RF bias of first, second and third harmonics. The partial power of beam P_{part} is determined according the following formula:

$$P_{part}(W) = \int_0^W \frac{\partial P}{\partial E}\, dE\,, \qquad (1)$$

where $\partial P/\partial E$ is differential power density of electron beam. The partial power is normalized on the total beam power $P_{tot}=P_{part}(W_{max})$, where W_{max} is the maximal beam energy.

One can notice that the additional RF biasing voltage can sufficiently reduce the low energy part of spectrum.

Figure 10 represents the calculated dependence of X-ray conversion efficiency [3] versus amplitude of RF biasing voltage at operating energy of 5 MeV and fixed beam power of 300 kW. This efficiency depends on electron energy spread, or, more precisely, on rate of low energy electrons in the spectrum.

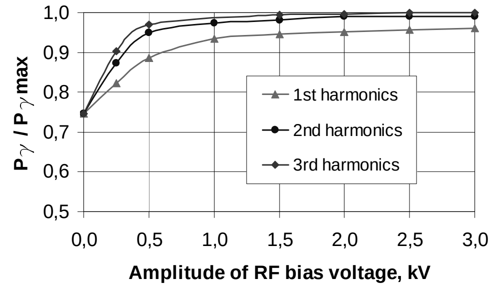

Figure 10: RF biasing voltage amplitude dependence of relative X-ray power for fixed beam power.

To prove the possibility to correct the electron energy spectrum by applying the RF biasing voltage to the cathode-grid gap the measurements were carried out on the existing linear RF accelerator ILU-10 [1] at energy of 5 MeV and beam power of 50 kW. Figure 11 represents the results of computer simulation and experimental data obtained on ILU-10 machine. The computer simulation model was not absolutely correct because the magnet lens of ILU-10 machine and real transverse size of the beam were not considered in the calculations, but the simulation and experimental results are in reasonable agreement. The experimental data proves that usage of RF biasing can really improve the electron beam energy spectrum.

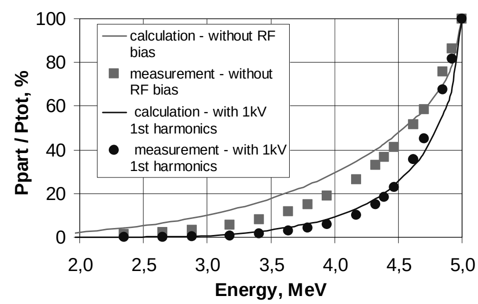

Figure 11: Electron beam energy spectrum of ILU-10 machine without and with RF bias voltage.

5 CONCLUSION

The results obtained proved the possibility to solve the main problems and so to create the efficient and powerful electron accelerator for energy of 5-10 MeV and beam power of 300 kW.

6 REFERENCES

[1] V. Auslender et al. Accelerators for E-beam and X-ray processing. Radiation Physics and Chemistry 63 (2002) pp. 613–615.
[2] B. Fomel et al. SAM – an interactive code for evaluation of electron guns. Preprint BINP 96-11.
[3] A. Bukin. Private communication.